PAPER

Ring-opening polymerization of ε-caprolactone by lithium piperazinyl-aminephenolate complexes: synthesis, characterization and kinetic studies†

Nduka Ikpo,[a] Christian Hoffmann,[a] Louise N. Dawe[a,b] and Francesca M. Kerton*[a]

A series of lithium complexes were prepared from 2(*N*-piperazinyl-*N'*-methyl)-2-methylene-4-R'-6-R-phenols ([ONN]$^{RR'}$) and characterized through elemental analysis, ^{1}H and ^{13}C{^{1}H} NMR spectroscopy, and X-ray crystallography. Treatment of the ligands with n-butyllithium afforded {Li[ONN]$^{RR'}$}$_3$ [R = Me, R' = ^{t}Bu, (**1**); R = R' = ^{t}Bu (**2**); R = R' = ^{t}Am, (**3**), ^{t}Am = C(CH$_3$)$_2$CH$_2$CH$_3$], with trimetallic structures in the solid-state as shown by single-crystal X-ray diffraction. The reactivity of these complexes in the ring-opening polymerization of ε-caprolactone (ε-CL), as well as the influences of monomer concentration, monomer/Li molar ratio, polymerization temperature and time, was studied. Rates of polymerization were first order with respect to both monomer and lithium concentrations, and activation energies for the reactions were determined. MALDI-TOF MS analysis revealed that transesterification had occurred during the polymerization.

Introduction

Aminephenolate and related ligands that possess a mixed set of *N*- and *O*-donor atoms have attracted a great deal of interest over the past decade mainly due to their ability to coordinate to a range of metal centres and the ease of systematic manipulation of their steric and electronic properties by variation of their backbone and phenol substituents.[1] Various ligands of this type have been used in main group and early transition metal chemistry (including lithium,[2–7] magnesium,[8–14] calcium,[15] rare-earths,[16,17] zinc,[18–27] aluminum,[28–30] zirconium[31,32] and titanium[33]). Many of these complexes have been reported to be excellent initiators for the ring-opening polymerization (ROP) of cyclic esters such as lactide and ε-caprolactone.

To date most well-characterized lithium aminephenolate complexes reported have contained bis(phenolate) ligands.[2–5,34–36] This contrasts with related mono-anionic aminephenolate lithium complexes that still remain relatively unexplored.[6] Furthermore, it has been established that lithium phenolates usually contain square Li$_2$O$_2$ dimers or 'daisy-chain' Li$_4$O$_4$ tetramers with μ$_2$-bridging-phenolate interactions. In the literature, very few structurally characterized trimetallic lithium phenolate complexes have been reported: [LiOC$_6$H$_2$(CH$_2$NMe$_2$)$_2$-2,6-Me-4]$_3$,[37] [LiOC$_6$H$_3${2,6(^{i}Pr)$_2$}(THF)]$_3$[38] and [{Li(OC$_6$H-3,5-^{t}Bu$_2$-2,6-Ph$_2$)}$_3$].[39]

Following our recently reported work on zinc compounds of piperazinyl aminephenolate ligands,[18] which efficiently initiated the ring-opening polymerization of *rac*-lactide and ε-caprolactone in a controlled manner, we decided to study the chemistry of related Li complexes. Herein, we report the synthesis and structural characterization of trimetallic lithium piperazinyl aminephenolate complexes. Their catalytic activities in ring-opening polymerization of ε-caprolactone in the presence and absence of benzyl alcohol were also investigated.

Results and discussion
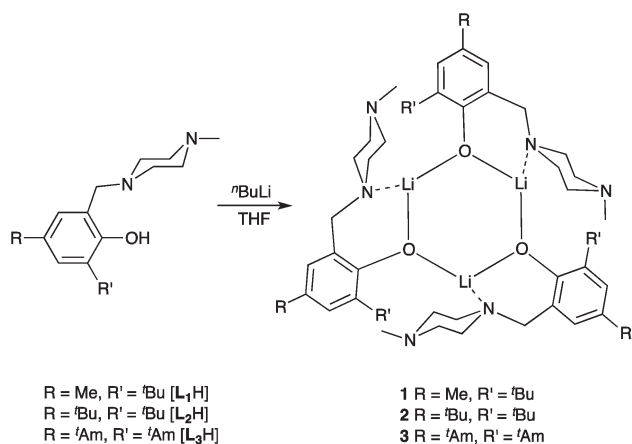
Synthesis and solid-state structures

The reactions of 1.1 equiv. of n-butyllithium with the appropriate protio ligands in THF at −78 °C gave the corresponding lithium methylpiperazinyl aminephenolate complexes {Li[ONN^{Me,tBu}]}$_3$, **1**, {Li[ONN^{tBu,tBu}]}$_3$, **2** and {Li[ONN^{tAm,tAm}]}$_3$, **3** in high yield (Scheme 1). Of the alkyl groups on the aromatic rings, the *tert*-amyl groups, also known as *tert*-pentyl, were the most sterically demanding used in this study (^{t}Am = C(CH$_3$)$_2$CH$_2$CH$_3$).

Single crystals of **1** suitable for X-ray diffraction analysis were obtained by cooling a saturated toluene–hexane solution to −35 °C. The molecular structure shown in Fig. 1 shows complex **1**, which is a trimetallic lithium complex with the lithium centres bridged by phenolate oxygen atoms to form a Li$_3$O$_3$ six-membered ring. The bridging oxygen atoms are *ca.* 0.37 Å off the mean plane of the three central lithium ions. The central ring O(1)–Li(1)–O(1′) and Li(1)–O(1)–Li(1′) angles are 121.09(14) and 110.93(14)° respectively, which sum to 693.03° for all internal angles of the six-membered ring indicating a deviation from a perfect plane of 720° by 26.97°. The structure possesses a pseudo-threefold rotation axis with each of the three-coordinate
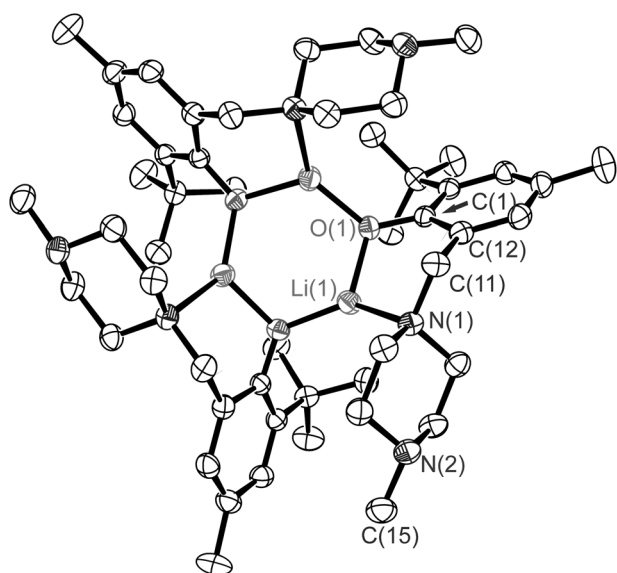
[a]*Department of Chemistry, Memorial University of Newfoundland, St. John's, NLA1B 3X7, Canada. E-mail: fkerton@mun.ca*
[b]*X-ray Crystallography Laboratory, C-CART, Memorial University of Newfoundland, St. John's, NLA1B 3X7, Canada*

Scheme 1

R = Me, R' = ^{t}Bu [L$_1$H]
R = ^{t}Bu, R' = ^{t}Bu [L$_2$H]
R = ^{t}Am, R' = ^{t}Am [L$_3$H]

1 R = Me, R' = ^{t}Bu
2 R = ^{t}Bu, R' = ^{t}Bu
3 R = ^{t}Am, R' = ^{t}Am

Fig. 1 Molecular structure of **1** (50% thermal ellipsoids; H atoms excluded for clarity). Selected bond lengths (Å) and bond angles (°): O(1)–C(1), 1.3358(16); O(1)–Li(1), 1.832(3); O(1)–Li(1), 1.844(3); N(1)–Li(1), 2.105(3); Li(1)–Li(1), 3.028(4); C(1)–O(1)–Li(1), 128.70(11); C(1)–O(1)–Li(1), 116.33(11); Li(1)–O(1), 110.93; O(1)–Li(1)–O(1), 121.09(14); O(1)–Li(1)–N(1), 132.81(14); O(1)–Li(1)–N(1), 101.30(11).

lithium ions adopting a distorted trigonal planar geometry. The C$_3$NLiO six-membered chelate ring adopts a boat conformation with C(12) and O(1) situated *ca.* 0.66 and 0.52 Å off the mean plane of Li(1)–C(1)–C(11)–N(1) respectively. The phenolate rings are tilted with respect to the plane containing the lithium centres such that they displayed a propeller-like arrangement whose directions are controlled by the coordinated amine of the ligand. The bond lengths Li(1)–O(1) [1.844(3) Å], Li–(1)–O(1) [1.832(3) Å], and Li(1)–N(1) [2.105(3) Å] are comparable to related trimetallic and bimetallic lithium complexes reported in the literature,[5,33,37–39] but shorter than those (Li–O [1.938(3)–2.096(4) Å] and Li–N [2.158(3)–2.213(3) Å]) found for bridged phenoxide.[34]

Crystals of complex **3** were also grown from toluene–hexane at −35 °C. The single crystal X-ray analysis shows that **3** crystallizes as a trimetallic species in the triclinic space group $P\bar{1}$ and is slightly less symmetric than **1** due to the greater steric demands of **L3** compared with **L1**, and thermal disorder within the *tert*-amyl groups. The structural features of each Li atom in complex **3** are similar to those in complex **1**, each Li adopts a distorted trigonal planar geometry with the three-coordinate metal centre coordinated to two phenolate oxygen donors and an amine nitrogen atom of the piperazinyl group. The angles around the metal centre and the bond lengths from the Li to the oxygen and nitrogen atoms are similar to those of complex **1**. Attempts to grow crystals of complex **2**, however, led to amorphous white precipitates. Complexes **1**–**3** were further characterized by elemental analysis, ^{1}H and ^{13}C{^{1}H} NMR spectroscopy. Variable temperature NMR studies of complexes **1**–**3** were recorded in C$_5$D$_5$N from −35 to 70 °C and showed sharp, readily assignable peaks for the methylene (PhCH$_2$N, NCH$_2$CH$_2$N) and amine methyl groups at elevated temperature. When the temperature was slowly decreased to ambient, the methylene peaks broadened and became indistinguishable from the spectral baseline. On further decreasing the temperature to below 0 °C, the methylene peaks became diastereotopic. The NMR spectral data for **1**–**3** are in good agreement with their formulations (Fig. S1†).

Ring-opening polymerization of ε-caprolactone

The ring opening polymerization (ROP) of ε-caprolactone (ε-CL) was performed using complexes **1**, **2** and **3** as catalysts in a toluene solution in the presence or absence of benzyl alcohol (BnOH). The complexes were highly reactive in the polymerization of ε-caprolactone as summarized in Table 1. The choice of solvent was made by surveying the solvent effect on the ROP of ε-caprolactone using **1**, and it was observed that when tetrahydrofuran (THF) was used instead of toluene the ROPs proceeded slightly more slowly (Table 1, entries 1–3). This could be attributed to the coordinating nature of THF, which competes with the incoming monomer for coordination at the metal centre. The use of alcohols as activators has been reported to be necessary for ROPs of cyclic esters.[2,4,6] In the current study, the polymerization time required in the absence of benzyl alcohol was longer than in the presence of benzyl alcohol as shown in Table 1, entries 9–18, 22–24. However, the reactions still proceeded. Theoretical number-average molecular weights (M_{ncal}) differed from the values obtained *via* GPC. Polydispersities increased with temperature (Table 1, entries 7, 8, 11, 12, 16, 17 and 21) and reaction time (Table 1, entries 6, 18, and 19). The polydispersity of all the polymerization reactions at or above 40 °C was high (>1.5), which suggests that transesterification had occurred. Also, it should be noted that the polydispersities are generally higher than those reported for poly(lactic acid) produced using lithium amine bis(phenolate) complexes.[4,6]

However, as it can be seen from Table 1, complex **3**, that contains the most sterically-demanding of the three ligands studied, in the presence of BnOH produces polymers with generally narrower polydispersity. This suggests that the polymerization reactions initiated by **3** proceeded in a more controlled fashion

Table 1 Polymerization of ε-CL using **1**, **2** and **3** in the presence and absence of BnOH[a]

Entry	Complex	$[CL]_0/[Li]_0/[BnOH]_0$	t/min	T/°C	Conv/%[c]	$M_{ncal}{}^d \times 10^3$	$M_n{}^e \times 10^3$	$M_w/M_n{}^e$
1	**1**	5011/0[b]	60	25	23.1	—	—	—
2	**1**	50/1/0[b]	30	60	92.6	5.28	6.80	2.19
3	**1**	100/1/0[b]	150	60	65.2	—	—	—
4	**1**	100/0/1	60	60	—	—	—	—
5	**1**	50/1/0	30	25	97.0	5.54	32.5	1.31
6	**1**	100/1/0	50	25	98.0	11.2	15.9	1.71
7	**1**	200/1/0	30	40	83.0	18.9	15.7	1.99
8	**1**	200/1/0	25	60	98.0	22.3	21.5	2.02
9	**1**	50/1/1	2	25	99.7	5.65	2.36	1.28
10	**1**	100/1/1	5	25	93.4	10.6	3.26	1.36
11	**1**	200/1/1	10	80	93.0	21.3	11.6	2.04
12	**1**	200/1/1	10	60	99.1	22.6	5.94	1.58
13	**1**	300/1/1	7	25	99.0	50.8	3.19	1.20
14	**2**	50/1/1	1	25	99.9	5.7	2.07	1.17
15	**2**	100/1/1	2	25	99.9	11.4	3.69	1.32
16	**2**	200/1/1	6	40	99.0	22.6	4.27	1.57
17	**2**	300/1/1	6	40	93.0	31.8	5.04	1.58
18	**3**	50/1/0	40	25	100	5.7	21.4	1.73
19	**3**	100/1/0	90	25	99.8	11.4	9.92	1.92
20	**3**	200/1/0	40	40	90.0	20.5	21.4	1.45
21	**3**	200/1/0	15	60	93.0	21.2	21.6	2.03
22	**3**	50/1/1	2	25	99.6	5.6	2.48	1.24
23	**3**	100/1/1	4	25	99.8	11.3	3.83	1.26
24	**3**	200/1/1	10	25	77	17.6	4.11	1.28

[a] Reactions performed in toluene using the mole ratios indicated at the temperature and for the time indicated above. [b] Reaction performed in THF. [c] Determined by ^{1}H NMR spectroscopy. [d] The M_{ncal} value of the polymer was calculated with $M_{ncal} = ([\varepsilon\text{-CL}]_0/[Li]_0) \times 114.14 \times$ conv. %. [e] The M_n value was calculated according to $M_n = 0.56M_n{}^{GPC}$, where $M_n{}^{GPC}$ was determined by GPC (chloroform), and is relative to polystyrene standards.
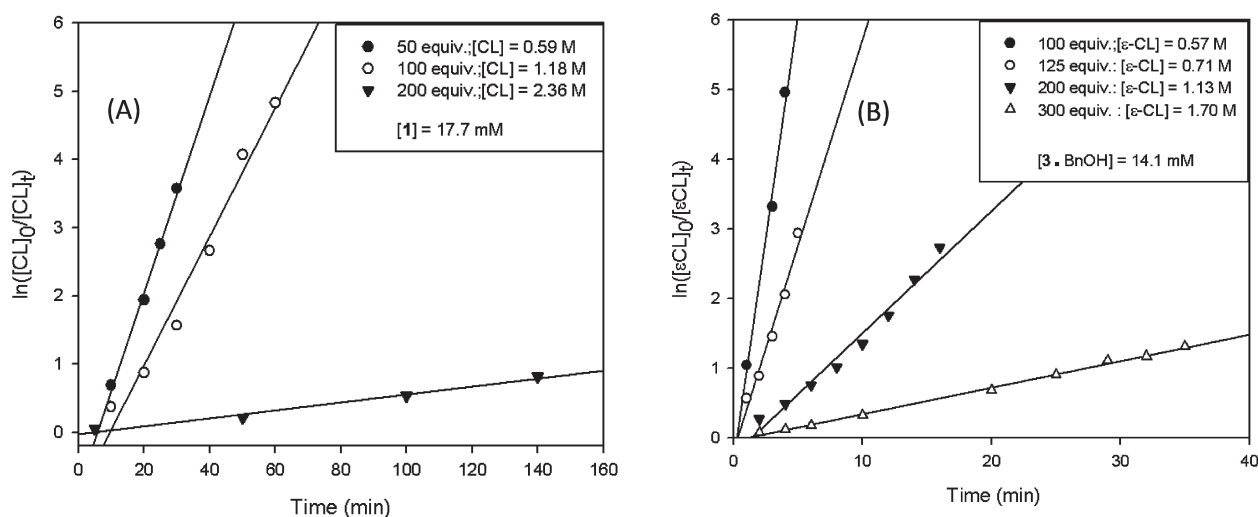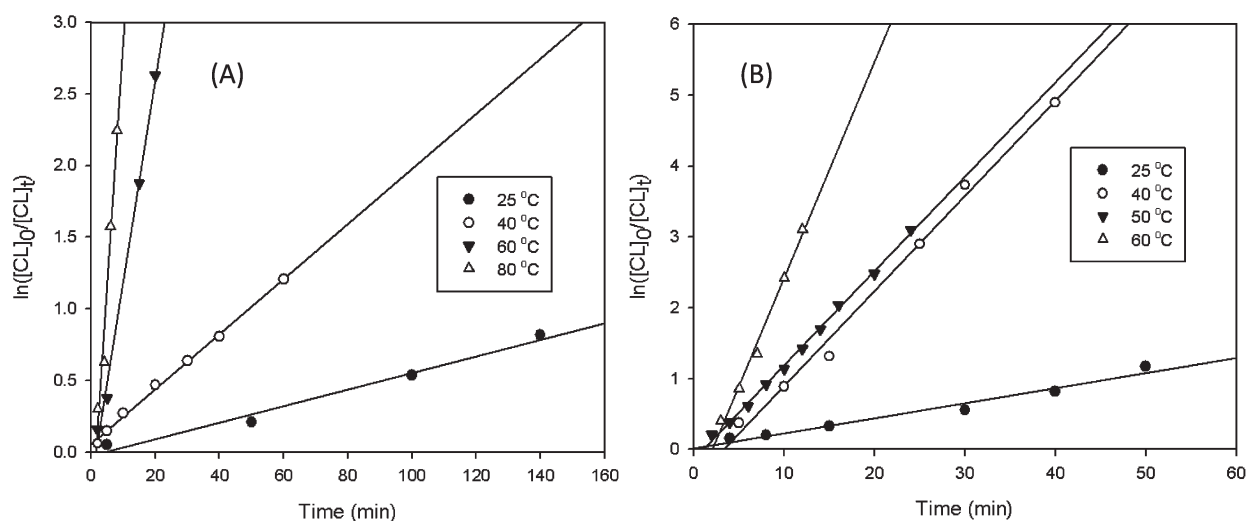

Fig. 2 Semilogarithmic plots of the monomer conversion stated as $\ln[CL]_0/[CL]_t$ *versus* the reaction time for the polymerization of ε-caprolactone at different monomer molar ratios using (a) **1**; $[CL]_0/[1]_0 = 50$ (●), 100 (○), 200 (▼) ($[1]_0 = 17.7$ mM, 25 °C) and (b) **3**-BnOH; $[CL]_0/[3\text{-BnOH}]_0 = 100$ (●), 125 (○), 200 (▼), 300 (△), ($[3\text{-BnOH}]_0 = 17.7$ mM, 34 °C).

and that the ligand remains coordinated to the metal centre throughout the process.

It should also be noted that gelation was observed during the preliminary polymerization reactions. This led us to investigate the effects of monomer concentration (solvent volume) on the reactions. As one would expect, running the reaction at dilute monomer concentration levels lowered the rate of the reaction and afforded low conversions (Fig. S2†). A similar trend was also observed by Thibault and Fontaine.[40]

Kinetic studies of ε-caprolactone polymerization

In order to better understand the nature of these ε-caprolactone polymerizations, a series of reactions were conducted in toluene at ambient temperature for various monomer to lithium $[CL]/[Li]$ ratios. The conversion of ε-caprolactone was monitored by ^{1}H NMR analysis and semilogarithmic plots of $\ln[CL]_0/[CL]_t$ *versus* time for two such polymerizations are shown in Fig. 2. The plots revealed linear relationships in each case, indicating a

Fig. 3 Semilogarithmic plots of the monomer conversion stated as $\ln[CL]_0/[CL]_t$ *versus* the reaction time for the polymerization of ε-caprolactone at different temperatures using (a) **1**; $[CL]_0/[1]_0 = 200$, ($[1]_0 = 17.7$ mM, $[CL] = 1.18$ M); (●) = 25, (○) = 40, (▼) = 60, (△) = 80 °C, and (b) **1**-BnOH; $[CL]_0/[1\text{-BnOH}]_0 = 200$, ($[1]_0 = 17.7$ mM, $[CL] = 1.18$ M); (●) = 25, (●) = 40, (▼) = 50, (△) = 60 °C.

first-order dependence of reaction rate on monomer concentration. In all semilogarithmic plots presented within this article, $R \geq 0.98$. Data points for each line were obtained from a single experiment and if $R < 0.98$, the experiment was repeated with the aim of obtaining more accurate data. Deviations from linearity result from experimental error including catalyst decomposition and inhomogeneous heating of the reaction mixture.

Further kinetic studies were carried out to determine the reaction rate (k_{obs}) and the effect of temperature at various reaction temperatures. It was observed that the overall polymerization rate increases with temperature (Fig. 3). The semilogarithmic kinetic plots for ε-caprolactone polymerization using **1** and **1**-BnOH are depicted in Fig. 3 and linear dependencies were found for $\ln[CL]_0/[CL]_t$ *versus* time for all polymerizations studied (Fig. S3 and S5† for **3** and **3**-BnOH).

The values for the observed rate constant (k_{obs}) determined for **1** and **3** in the presence or absence of BnOH are summarized in Table 2 and are compared with values determined for various metal alkoxides. Unfortunately, for related amine-bis(phenolate) lithium complexes, and their activity in ROP of lactide, rate constants were not reported,[4,6] and therefore, a direct comparison cannot be made. It can be seen that the fastest polymerization was observed for **3**-BnOH, which is twice that for **1**-BnOH and lower than that of an yttrium phenolate complex (entry 5) and multi-metallic zinc species (entry 4), but is higher than that for the zinc, lanthanide and aluminum species (entries 1–3) shown in Table 2 for comparison.[41–45] Solvent appears to have some impact on the reported rates in the literature with significantly higher rates for the reactions performed in CH₂Cl₂ (entries 4 and 5) compared with toluene. The rates for the reactions reported herein are therefore best compared with entries 1–3. The complexes used in entries 1–3 are known to perform ROP of lactones *via* coordination insertion mechanisms and the k_{obs} reported are of a similar order of magnitude to those seen in our studies. We propose that k_{obs} (entries 6 and 8) in the presence of BnOH were greater than in the absence of alcohol for two reasons. First, the resulting benzyl alkoxide group is a better nucleophile than the

Table 2 A comparison of rate constants for ε-caprolactone polymerization by various metal alkoxides

| Entry	Metal complex	Solvent	$T/°C$	$k_{obs}/\text{L mol}^{-1}\text{min}^{-1}$	Ref.
1	La(OTBP)$_3$[a]	Toluene	60	0.186	41
2	Me$_2$Al[O-2-^{t}Bu-6 $\{(C_6F_5)N\!=\!CH\}C_6H_4]$/ BnOH	Toluene	50	0.028	42
3	Et$_2$AlO(CH$_2$)$_3$CH$=$CH$_2$	Toluene	0	0.16	43
4	[{(BDI-OMe)Zn (μ-OBn)}$_2$Zn(μ-OBn)$_2$]	CH$_2$Cl$_2$	25	97.2	44
5	(RO)$_3$Y[b]	CH$_2$Cl$_2$	22	1.65	45
6	{Li[ONN^{Me,tBu}]}$_3$ (**1**)	Toluene	40	0.019	This work
7	{Li[ONN^{Me,tBu}]}$_3$ (**1**)/ BnOH	Toluene	40	0.133	This work
8	{Li[ONN^{tAm,tAm}]}$_3$ (**3**)	Toluene	40	0.036	This work
9	{Li[ONN^{tAm,tAm}]}$_3$ (**3**)/ BnOH	Toluene	40	0.273	This work

[a] Lanthanum tris(4-*tert*-butylphenolate). [b] Yttrium 2,6-di-*tert*-butyl-phenoxide and isopropanol.

aryloxide ligand. This means that the ring-opening step (likely the rate-determining step) occurs more rapidly. Secondly, the presence of BnOH would assist in disassembly of Li-aggregates present in solution. As reaction rates are dependent on the ligand employed, the ligand must remain coordinated to the Li centre throughout the polymerization process, Scheme 2.

An Arrhenius analysis showed that the relationship between the rate constants (k_{obs}) and the polymerization temperature was in good agreement with the Arrhenius equation. From Fig. 4, S4 and S6† the activation energies (E_a) of ε-caprolactone polymerization by **1** and **3** in the absence and presence of BnOH were determined. Unfortunately, we were unable to find data for related ROP reactions using lithium complexes in the literature and therefore, comparison is made with other discrete metal complexes used in ROP of ε-caprolactone. The value of E_a obtained for **1** in the absence of BnOH [67.2 ± 1.0 kJ mol^{-1}]
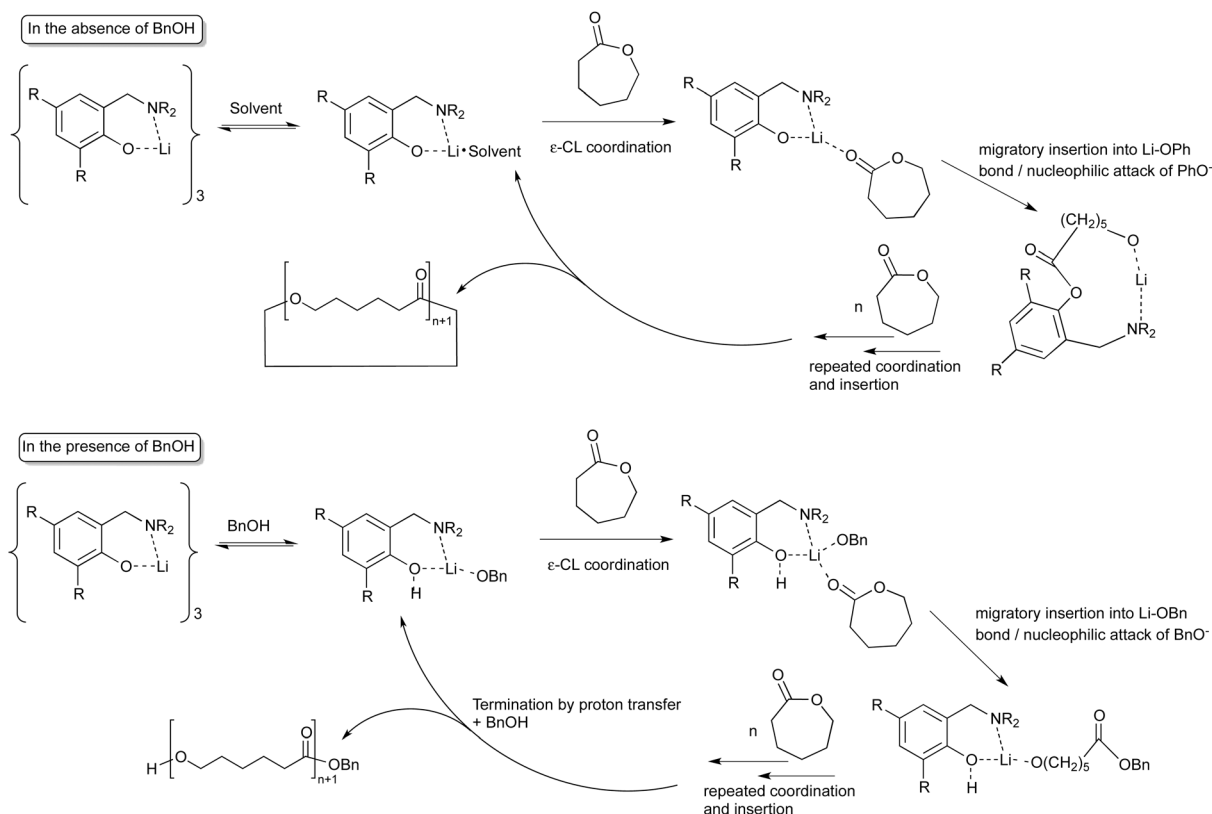
Scheme 2 Proposed mechanism for catalytic ROP of ε-caprolactone using Li aminephenolate complexes. Ligand has been simplified for clarity.
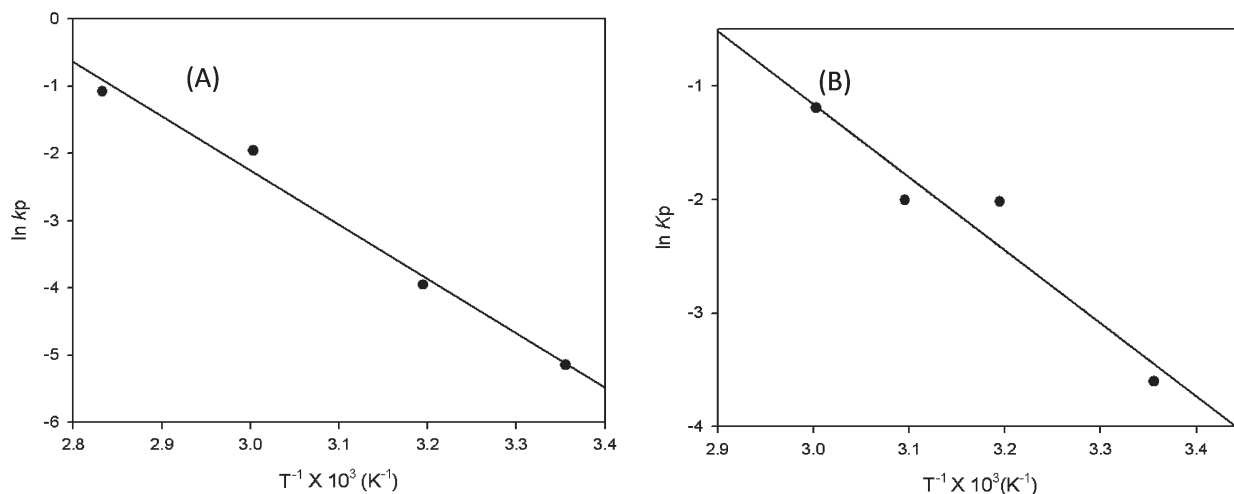
Fig. 4 Arrhenius plots of $\ln(k_{obs})$ *vs.* $1/T$ for the ring-opening polymerization of ε-caprolactone using (A) **1**:[**1**] = 17.7 mM; [CL]/[**1**] = 200; $R = 0.9927$, $R^2 = 0.9855$, and (B) **1**-BnOH; [**1**-BnOH]$_0$ = 17.7 mM; [CL]/[**1**] = 200; $R = 0.9609$, $R^2 = 0.9233$.

is higher than those obtained for ROP of ε-caprolactone catalyzed by scandium aryloxide [58.0 kJ mol^{-1}],[46] lanthanide tris-(4-*tert*-butylphenolate) [51.9 kJ mol^{-1}],[41] lanthanide tris(2,4,6-tri-*tert*-butylphenolate) [39.3 kJ mol^{-1}],[47] and titanium dialkano-lateamine [48.5 kJ mol^{-1}].[48] However, in the presence of BnOH, the determined value [53.4 ± 4.1 kJ mol^{-1}] is similar to many of the values reported in the literature. The values determined for **3** in the absence of BnOH [56.8 ± 1.2 kJ mol^{-1}] and in the presence of BnOH [48.8 ± 4.0 kJ mol^{-1}] are lower than those

determined for **1** and **1**-BnOH. Comparison of **1** and **3** using rate constants (Table 2) and activation energies indicate, under identical polymerization conditions, higher activity for **3** relative to **1**. These results indicate that changing the R substituents from *tert*-butyl (**1**) to the more sterically-demanding *tert*-amyl (**3**) enhanced polymerization rate and lowered the activation energy of the ROP of ε-caprolactone. These data support the coordination of the aminephenol(ate) ligand to the metal centre throughout the polymerization process, Scheme 2. The lower
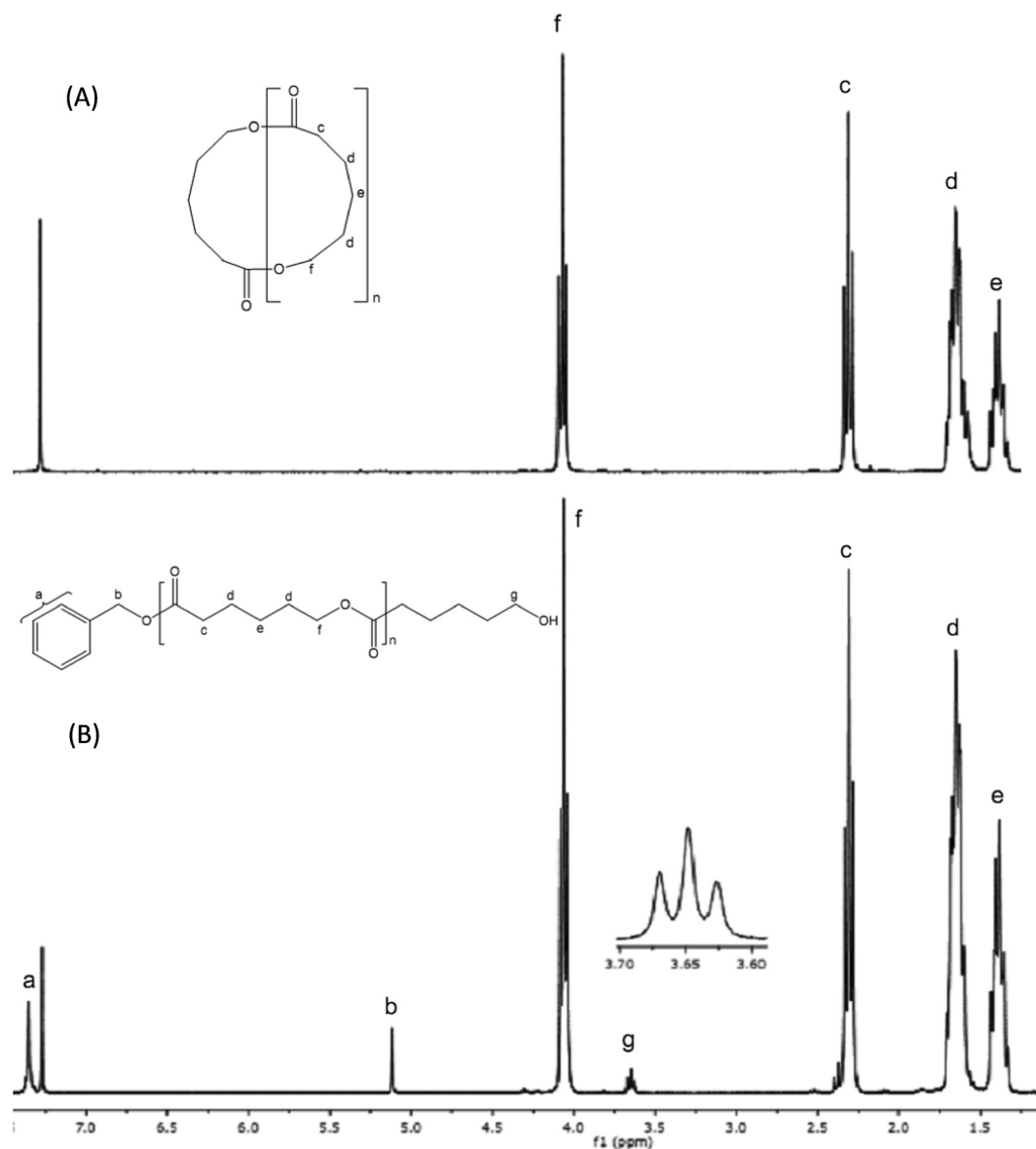
Fig. 5 Typical ^{1}H NMR spectra of PCL synthesized with: (A) **3** (Table 1, entry 18) and (B) **2**-BnOH (Table 1, entry 15).

E_a value for **3** might be indicative of easier dissociation of aggregated Li species in solution for the bulkier complexes but might also be the result of more electron rich Li centres for **3** compared with **1**.

NMR spectroscopy analysis of polycaprolactone

End-group analysis, by ^{1}H NMR spectroscopy, of the polymer obtained in the absence of BnOH shows typical polycaprolactone methylene proton signals at 1.38, 1.65, 2.31 and 4.06 ppm (Fig. 5(A)). However, no signals could be assigned to any end group and this suggests that the polymers obtained were cyclic polycaprolactone (as shown in Scheme 2). Furthermore, the ^{1}H NMR spectrum of the polymers prepared in the presence of BnOH displayed characteristic signals of polycaprolactone methylene protons (c–f) (Fig. 5(B)). Alongside these were resonances at 7.35 ppm (a) and 5.12 ppm (b) assigned to the benzyl

ester group, while the signal at 3.65 ppm corresponded to the hydroxymethylene ($–CH_2OH$) group (as shown in Scheme 2). ^{13}C NMR analysis confirmed the end-group assignments with the resonances of CH_2OH and OCH_2Ph appearing at 62.65, 66.18 and 128.58 ppm respectively (Fig. S7†). The signal assignments are in good agreement with previously reported results.[49] The presence of terminal benzyloxy and hydroxyl groups indicates that the ring-opening polymerization likely occurred through a coordination–insertion mechanism with the hydroxyl group introduced into the chain only at the termination stage. The proton could be transferred from the ligand (Scheme 2) or from the methanol used to quench the reaction.

MALDI-TOF MS analysis

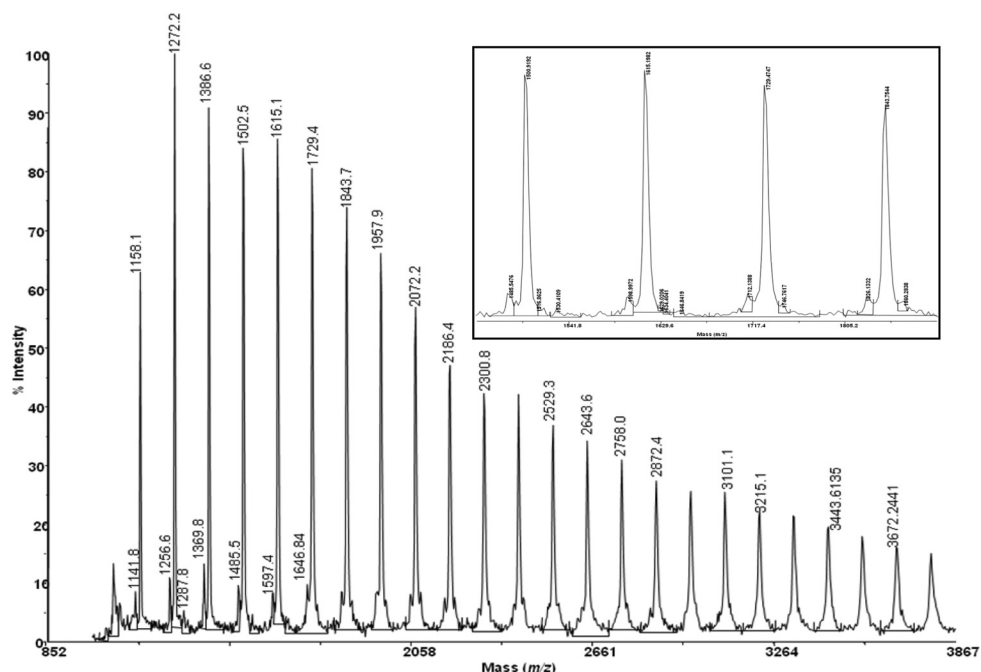The MALDI-TOF mass spectrum of the polycaprolactone prepared using complex **3** in the absence of BnOH is shown in

Fig. 6 MALDI-TOF mass spectrum of PCL from ROP using **3** in toluene at 40 °C, [CL]/[**3**] = 50 (Table 1, entry 18).

Fig. 6 (Table 1, entry 18). Three series of signals can be distinguished from the spectrum. The first minor series of peaks starting at the *m/z* 1141.8, 1303.0 *etc.* were attributed to cyclic oligomers, while the second major series at the *m/z* of 1158.1, 1272.2, 1386.6 correspond to open chain oligomers with hydroxy end group and the last minor peaks were assigned to cyclic oligomers clustered with Na⁺. The analysis of successive series shows that there is a difference of 114 in *m/z* between every neighbour in each series, which corresponds to the molecular weight of ε-caprolactone. It was also observed that successive peaks in the major series exhibit both even-membered and odd-membered oligomers. Interestingly, all the polymer samples obtained with **1**, **2** and **3** in the absence of BnOH showed similar series of species (Fig. S8–S9†). It is well known that an odd–even distribution is a characteristic of intramolecular esterification (back-biting) reactions at long reaction times and at high conversion levels, and that this leads to the formation of cyclic oligomers.[50] Therefore, the presence of the odd–even oligomers in the MALDI-TOF mass spectra indicate that transesterification occurred during the polymerization reactions reported herein.

Furthermore, the MALDI-TOF mass spectrum of the polymer prepared with **2** in the presence of BnOH (Table 1, entry 15, Fig. S10–S13†) as depicted in Fig. 7 revealed the presence of four populations. Three minor peak populations of PCL with minimal intensity from the low *m/z* region of the spectrum were identified as related to macromolecules capped with (a) BnO group (BnO{CL}$_n$H), (b) clustered with Na⁺ (BnO{CL}$_n$H)Na⁺ and (c) K⁺ adducts (BnO{CL}$_n$H)K⁺ respectively. The main signals (most important signals) of the mass spectrum are separated by a caprolactone unit (114 g mol⁻¹) and correspond to polymer chain terminated with hydroxy and BnO end-groups, (BnO{CL}$_n$OH). The identification of PCL capped with BnO

and hydroxyl end-groups as the main signals in the MALDI-TOF mass spectrum is in agreement with ¹H NMR analysis and confirms that the polymerization occurred through a coordination–insertion mechanism.

It is worth noting that even though the polydispersity seems not to be affected and remains fairly narrow in most cases, it can be seen that oligomers appear from the very start of the polymerization process, which is an indication of intermolecular transesterification. Dubois *et al.*[51] reported that the occurrence of inter- and intramolecular transesterification reactions can produce broadening of the polydispersity, a decrease in the average molecular weight and the appearance of a soluble low molecular weight fraction. This probably can explain the observed disparity in the calculated and experimental average molecular weight from both GPC and MALDI-TOF mass spectrometric data. MALDI-TOF mass spectra of polycaprolactone formed using Li–phenolate complexes have not been reported previously. Therefore, comparison was made with data reported using other metal complexes. In all the MALDI spectra of the polycaprolactone studied, the signals are similar to polymers obtained with tin(II) octoate or ammonium decamolybdate (NH$_4$)$_8$[Mo$_{10}$O$_{34}$] in the presence of alcohol or water.[52–54]

Conclusion

In summary, novel trimetallic lithium complexes supported by monoanionic piperazinyl aminephenolate ligands were synthesized and their structure features characterized by X-ray diffraction studies. Polymerization studies showed that the complexes could efficiently perform the ring-opening polymerization of ε-caprolactone. The results of kinetic studies revealed a first order dependence on monomer. Polymer end-group analysis
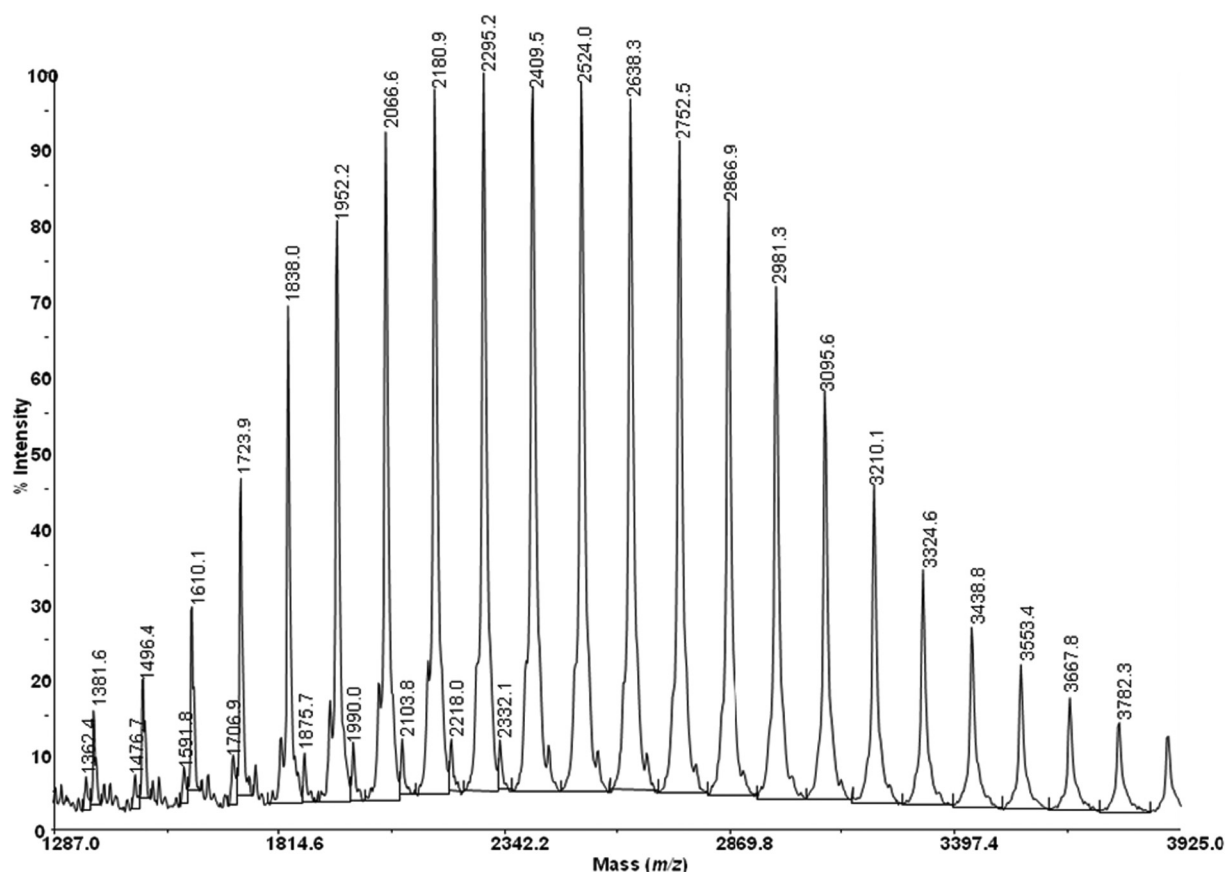
Fig. 7 MALDI-TOF mass spectrum of PCL formed using **2**-BnOH in toluene at 25 °C, [CL]/[**2**] = 100 (Table 1, entry 15).

by ^1H NMR, ^{13}C NMR and MALDI-TOF MS, when reactions had been conducted in the presence of BnOH, showed that the benzyloxide group was incorporated into the polycaprolactone growing chain. This supports the coordination–insertion mechanism seen by others. In addition, polymerization in the absence of BnOH led to cyclic and open chain oligomer formation indicating that the ROPs were accompanied by transesterification reactions.

Experimental

General

All experiments involving metal complexes were performed under a nitrogen atmosphere using standard Schlenk and glovebox techniques. Solvents were distilled under nitrogen over sodium–benzophenone (THF, toluene, hexane) and degassed by freeze–vacuum–thaw cycles prior to use. Deuterated solvents (C_6D_6, $CDCl_3$, C_5D_5N) were purchased from Cambridge Isotope Laboratories, Inc. and purified and dried before use. 2,4-Di(*tert*-butyl)phenol, 2-*tert*-butyl-4-methylphenol, 2,4-di(*tert*-amyl) phenol, n-butyllithium and 1-methylpiperazine were purchased from Alfa Aesar. Elemental analyses were performed by Canadian Microanalytical Service Ltd., Delta, BC, Canada. ^1H and $^{13}C\{^1H\}$ NMR spectra were recorded on a Bruker Avance 500 or 300 MHz spectrometer at 25 °C (unless otherwise stated) and were referenced internally using the residual proton and ^{13}C

resonances of the solvent. ^{13}C signals were assigned using HSQC experiments. ^7Li NMR was recorded on a Bruker 300 MHz spectrometer and referenced externally to LiCl in D_2O. For the polymers, mass spectrometric measurements were performed using an Applied Biosystems 4800 TOF-TOF instrument and mass spectra were recorded in linear mode. 2-(4-Hydroxy-phenylazo)benzoic acid (HABA) was used as the matrix and purified tetrahydrofuran was used as the solvent for depositing analytes onto the instrument's plate. GPC data were collected on a Viscotek GPCMax System equipped with a Refractive Index Detector (Phenogel 5 μ linear/mixed bed 300 × 4.60 mm column in series with a Phenogel 5 μ, 100 Å, 300 × 4.60 mm column). Samples were run in chloroform at a concentration of 1 mg mL^{-1} at 35 °C. The instrument was calibrated against polystyrene standards (Viscotek) to determine the molecular weights (M_n and M_w) and the polydispersity index (M_w/M_n) of the polymers. Conversions were determined by integration of the ε-methylene signals due to the residual ε-CL and poly-(ε-caprolactone).

Single crystal X-ray diffraction studies. Crystals of **1** and **3** were mounted on low temperature diffraction loops and measured on a Rigaku Saturn CCD area detector with graphite monochromated Mo-Kα radiation. Structures were solved by direct methods[55,56] and expanded using Fourier techniques.[57] Neutral atom scattering factors were taken from Cromer and Waber.[58] Anomalous dispersion effects were included in F_{calc}[59]

Table 3 Summary of crystal data for compounds **1** and **3**[a]

Compounds	1	3
Formula	$C_{51.50}H_{83}Li_3N_6O_{3.50}$	$C_{66}H_{111}Li_3N_6O_3$
Formula weight	863.08	1057.46
Crystal system	Trigonal	Triclinic
Space group	$R\bar{3}$	$P\bar{1}$
$a/\text{Å}$	19.315(2)	9.905(2)
$b/\text{Å}$	19.315(2)	18.234(5)
$c/\text{Å}$	24.872(3)	20.026(6)
$\alpha/°$	90	107.574(3)
$\beta/°$	90	103.944(5)
$\gamma/°$	120	90.860(5)
$V/\text{Å}^3$	8036.0(17)	3331.4(15)
T/K	153	153
Z	6	2
$D_c/\text{g cm}^{-3}$	1.070	1.054
$F(000)$	2826	1164
$\mu(\text{Mo-K}\alpha)/\text{cm}^{-1}$	0.66	0.63
Total reflections	34 847	32 540
Unique reflections	3697 ($R_{int} = 0.0240$)	13 769 ($R_{int} = 0.0313$)
No. of observations	3697	13 769
No. of parameters	198	749
R_1 ($I > 2.00\sigma(I)$)	0.0589	0.1008
wR_2	0.1677	0.2940
GOF	1.084	1.104

[a] Data in common: graphite-monochromated *via* Rigaku SHINE Optic Mo-Kα radiation, $\lambda = 0.71073$ Å; $R_1 = \Sigma||F_o| - |F_c||/\Sigma|F_o|$, $wR_2 = [\Sigma(w(F_o^2 - F_c^2)^2)/\Sigma w(F_o^2)^2]^{1/2}$ $w^{-1} = [\sigma^2(F_o^2) + (aP)^2$, $P = [\text{Max}(F_o^2, 0) + 2(F_c^2)]/3$.

the values for $\Delta f'$ and $\Delta f''$ were those of Creagh and McAuley.[60] The values for the mass attenuation coefficients are those of Creagh and Hubbell.[61] All calculations were performed using CrystalStructure[62,63] except for refinement, which was performed using SHELXL-97.[64] Non-hydrogen atoms were refined anisotropically, unless otherwise indicated, while hydrogen atoms were introduced in calculated positions and refined on a riding model (Table 3).

For **1**, the asymmetric unit contains a 1/6-occupancy methanol molecule adjacent to a special position. This molecule was refined isotropically, and the corresponding protons could not be located from difference maps, and were therefore omitted from the model. For **3**, C(32A, 33–35 and 36A) (0.25 occupancy) and C(32B, 36B and 37–39) (0.75 occupancy) make up two parts of a disordered amyl group. Similarity restraints were applied to these disorder components, and sensible anisotropic convergence was achieved.

Synthetic procedures

{Li[ONN^{Me,tBu}]}$_3$ (1). A solution of n-butyllithium (6.50 mL, 10.0 mmol) in hexane was added dropwise to a stirred solution of **L1**H (2.5 g, 9.0 mmol) in THF (60.00 mL) at −78 °C. After stirring for 3 h, the solution was allowed to warm up to room temperature and stirred for a further 15 h. The solvent was then removed under vacuum to give a white residue. The residue was washed with cold pentane (20.00 mL), filtered and dried under vacuum to afford a white powder. Yield (2.46 g, 96%). Anal. Calc for $C_{51}H_{81}Li_3N_6O_3$: C, 72.32; H, 9.64; N, 9.92. Found: C, 72.10; H, 10.08; N, 9.30%. ^{1}H NMR (C_5D_5N, 500 MHz, 348 K) δ 7.35 (1H, s, Ar*H*), 7.00 (1H, s, Ar*H*), 3.75 (2H, s,

Ar–C*H$_2$*–N), 2.69 (4H, s, N–C$_2$*H$_4$*–C$_2$*H$_4$*–N), 2.45 (3H, s, NC*H$_3$*), 2.30 (4H, s, N–C$_2$*H$_4$*–C$_2$*H$_4$*–N), 2.12 (3H, s, ArC–C*H$_3$*), 1.76 (9H, s, ArC–C{C*H$_3$*}$_3$). ^{13}C{^{1}H} NMR (C_5D_5N, 125 MHz, 298 K): δ 150.4 (Ar*C*–O), 136.0 (Ar*C*–C{CH$_3$}$_3$), 129.7 (Ar*C*H), 128.9 (Ar*C*H), 126.0 (Ar*C*–CH$_2$N), 124.0 (Ar*C*–CH$_3$), 63.5 (ArC–*C*H$_2$–N), 54.5 (N–*C*H$_2$–CH$_2$–N), 54.4 (N–CH$_2$–*C*H$_2$–N), 46.2 (*C*H$_3$–N), 35.8 (ArC–*C*{CH$_3$}$_3$), 31.0 (ArC–C{*C*H$_3$}$_3$), 21.5 (ArC–*C*H$_3$). ^{7}Li NMR (C_5D_5N, 116 MHz, 298 K) δ 8.27.

{Li[ONN^{tBu,tBu}]}$_3$ (2). This compound was prepared in the same manner as described above for **1** with **L2**H (2.5 g, 7.85 mmol) and n-butyllithium (5.40 mL, 8.63 mmol) as starting materials. The product (2.3 g, 90%) was isolated as a white solid. Anal. Calc for $C_{60}H_{99}Li_3N_6O_3$: C, 74.04; H, 10.25; N, 8.63. Found: C, 74.24; H, 10.04; N, 8.82%. ^{1}H NMR (C_5D_5N, 500 MHz, 328 K) δ 7.62 (1H, s, Ar*H*), 7.14 (1H, s, Ar*H*), 3.69 (2H, s, Ar–C*H$_2$*–N), 2.65 (4H, s, N–C$_2$*H$_4$*–C$_2$*H$_4$*–N), 2.30 (4H, s, N–C$_2$*H$_4$*–C$_2$*H$_4$*–N), 2.10 (3H, s, C*H$_3$*–N), 1.83 (9H, s, ArC–C{C*H$_3$*}$_3$), 1.52 (9H, s, ArC–C{C*H$_3$*}$_3$); ^{13}C{^{1}H} NMR (C_5D_5N, 125 MHz, 298 K): δ 150.5 (Ar*C*–O), 136.8 (Ar*C*–C{CH$_3$}$_3$), 129.9 (Ar*C*H), 128.5 (Ar*C*H), 127.6 (Ar*C*–CH$_2$N), 124.0 (Ar*C*–C{CH$_3$}$_3$), 63.7 (ArC–*C*H$_2$–N), 54.5 (N–*C$_2$H$_4$*–C$_2$H$_4$–N), 54.4 (N–C$_2$H$_4$–*C$_2$H$_4$*–N), 46.2 (*C*H$_3$–N), 36.1 (ArC–*C*{CH$_3$}$_3$), 34.3 (ArC–*C*{CH$_3$}$_3$), 32.7 (ArC–C{*C*H$_3$}$_3$), 31.0 (ArC–C{*C*H$_3$}$_3$). ^{7}Li NMR (C_5D_5N, 116 MHz, 298 K) δ 8.22.

{Li[ONN^{tAm,tAm}]}$_3$ (3). This compound was prepared in the same manner as described above for **1** with **L3**H (2.8 g, 8.1 mmol) and n-butyllithium (5.60 mL, 8.9 mmol) as starting materials. The product (2.75 g, 97%) was obtained as a white solid. Anal. Calc for $C_{66}H_{111}Li_3N_6O_3$: C, 74.96; H, 10.58; N, 7.95. Found: C, 75.25; H, 10.38; N, 7.96%. ^{1}H NMR (C_5D_5N, 500 MHz, 328 K) δ 7.47 (1H, s, Ar*H*), 7.15 (1H, s, Ar*H*), 3.76 (2H, s, ArC–C*H$_2$*–N), 2.70 (4H, br, N–C$_2$*H$_4$*–C$_2$*H$_4$*–N), 2.37 (4H, br, N–C$_2$*H$_4$*–C$_2$*H$_4$*–N), 2.29 (2H, br, ArC–C–C*H$_2$*CH$_3$), 2.11 (3H, s, C*H$_3$*–N), 1.82 (2H, br, ArC–C–C*H$_2$*CH$_3$), 1.71 (6H, s, ArC–C{C*H$_3$*}$_2$), 1.47 (6H, s, ArC–C{C*H$_3$*}$_2$), 0.94 (3H, br, ArC–C–CH$_2$C*H$_3$*), 0.85 (3H, br, ArC–C–CH$_2$C*H$_3$*). ^{13}C{^{1}H} NMR (C_5D_5N, 125 MHz, 298 K): δ 150.5 (Ar*C*–O), 135.0 (Ar*C*–C–CH$_2$CH$_3$), 128.4 (Ar*C*H), 126.1 (Ar*C*H), 124.3 (Ar*C*–CH$_2$–N), 124.0 (Ar*C*–C–CH$_2$CH$_3$), 63.1 (ArC–*C*H$_2$–N), 54.2 (N–*C$_2$H$_4$*–C$_2$H$_4$–N), 54.1 (N–C$_2$H$_4$–*C$_2$H$_4$*–N), 46.2 (*C*H$_3$–N), 39.3 (ArC–*C*–CH$_2$CH$_3$), 38.1 (ArC–*C*–CH$_2$CH$_3$), 37.4 (ArC–*C*{CH$_3$}$_2$), 33.6 (ArC–C{*C*H$_3$}$_2$), 29.7 (ArC–C–*C*H$_2$CH$_3$), 28.7 (ArC–C–*C*H$_2$CH$_3$), 10.5 (ArC–C–CH$_2$*C*H$_3$), 10.0 (ArC–C–CH$_2$*C*H$_3$). ^{7}Li NMR (C_5D_5N, 116 MHz, 298 K) δ 8.19.

Typical polymerization procedure

All manipulations were performed under an inert atmosphere. The reaction mixtures were prepared in a glove box and subsequent operations were performed using standard Schlenk techniques.

A sealable Schlenk flask equipped with a stir bar was charged with a solution of complex **1** (10.0 mg, 35.4 μmol) in toluene (2.0 mL). Another Schlenk flask was charged with a toluene (6.0 mL) solution of ε-caprolactone (0.40 g, 3.54 mmol, 100 equiv.). The two flasks were then attached to a Schlenk line and

temperature equilibration was ensured in both Schlenk flasks by stirring the solutions for 10 min in a temperature controlled oil bath. The complex solution was transferred to the monomer solution that was stirring rapidly and polymerization times were measured from that point. At appropriate time intervals, aliquots of the reaction mixture were removed using a pipette for determining monomer conversion by ^{1}H NMR spectroscopy. The reaction was quenched with methanol once near-quantitative conversion had been obtained. The polymer was precipitated with an excess of cold methanol. The polymer was isolated by filtration and dried under reduced pressure.

Acknowledgements

References

1 O. Wichmann, R. Sillanpää and A. Lehtonen, *Coord. Chem. Rev.*, 2012, **256**, 371.
2 Y. Huang, Y.-H. Tsai, W.-C. Hung, C.-S. Lin, W. Wang, J.-H. Huang, S. Dutta and C.-C. Lin, *Inorg. Chem.*, 2010, **49**, 9416.
3 L. Wang, X. Pan, L. Yao, N. Tang and J. Wu, *Eur. J. Inorg. Chem.*, 2011, 632.
4 C.-A. Huang and C.-T. Chen, *Dalton Trans.*, 2007, 5561.
5 F. M. Kerton, C. M. Kozak, K. Luttgen, C. E. Willans, R. J. Webster and A. C. Whitwood, *Inorg. Chim. Acta*, 2006, **359**, 2819.
6 C.-A. Huang, C.-L. Ho and C.-T. Chen, *Dalton Trans.*, 2008, 3502.
7 B. Ko and C. Lin, *J. Am. Chem. Soc.*, 2001, **123**, 7973.
8 J. Ejfler, K. Krauzy-Dziedzic, S. Szafert, L. B. Jerzykiewicz and P. Sobota, *Eur. J. Inorg. Chem.*, 2010, 3602.
9 X. Zhang, T. J. Emge and K. C. Hultzsch, *Organometallics*, 2010, **29**, 5871.
10 A. D. Schofield, M. L. Barros, M. G. Cushion, A. D. Schwarz and P. Mountford, *Dalton Trans.*, 2009, 85.
11 W.-C. Hung and C.-C. Lin, *Inorg. Chem.*, 2009, **48**, 728.
12 L. E. Breyfogle, C. K. Williams, J. V. G. Young, M. A. Hillmyer and W. B. Tolman, *Dalton Trans.*, 2006, 928.
13 E. L. Marshall, V. C. Gibson and H. S. Rzepa, *J. Am. Chem. Soc.*, 2005, **127**, 6048.
14 Y. Sarazin, V. Poirier, T. Roisnel and J.-F. Carpentier, *Eur. J. Inorg. Chem.*, 2010, 3423.
15 D. J. Darensbourg, W. Choi, O. Karroonnirun and N. Bhuvanesh, *Macromolecules*, 2008, **41**, 3493.
16 H. E. Dyer, S. Huijser, A. D. Schwarz, C. Wang, R. Duchateau and P. Mountford, *Dalton Trans.*, 2008, 32.
17 A. Amgoune, C. M. Thomas and J. Carpentier, *Macromol. Rapid Commun.*, 2007, **28**, 693.
18 N. Ikpo, L. N. Saunders, J. L. Walsh, J. M. B. Smith, L. N. Dawe and F. M. Kerton, *Eur. J. Inorg. Chem.*, 2011, 5347.
19 V. Poirier, T. Roisnel, J. Carpentier and Y. Sarazin, *Dalton Trans.*, 2011, **40**, 523.
20 L. Wang and H. Ma, *Dalton Trans.*, 2010, **39**, 7897.
21 G. Labourdette, D. J. Lee, B. O. Patrick, M. B. Ezhova and P. Mehrkhodavandi, *Organometallics*, 2009, **28**, 1309.
22 J. D. Farwell, P. B. Hitchcock, M. F. Lappert, G. A. Luinstra, A. V. Protchenko and X. Wei, *J. Organomet. Chem.*, 2008, **693**, 1861.
23 J. Ejfler, S. Szafert, K. Mierzwicki, L. B. Jerzykiewicz and P. Sobota, *Dalton Trans.*, 2008, 6556–6562.
24 D. J. Doyle, V. C. Gibson and A. J. P. White, *Dalton Trans.*, 2007, 358.
25 C. K. Williams, L. E. Breyfogle, S. K. Choi, W. Nam, V. G. Young, M. A. Hillmyer and W. B. Tolman, *J. Am. Chem. Soc.*, 2003, **125**, 11350.
26 C. K. Williams, N. R. Brooks, M. A. Hillmyer and W. B. Tolman, *Chem. Commun.*, 2002, 2132.
27 M. H. Chisholm, J. C. Gallucci, H. Zhen and J. C. Huffman, *Inorg. Chem.*, 2001, **40**, 5051.
28 M. H. Chisholm and Z. P. Zhou, *J. Mater. Chem.*, 2004, **14**, 3081.
29 J. Lewinski, P. Horeglad, M. Dranka and I. Justyniak, *Inorg. Chem.*, 2004, **43**, 5789.
30 J.-T. Issenhuth, J. Pluvinage, R. Welter, S. Bellemin-Laponnaz and S. Dagorne, *Eur. J. Inorg. Chem.*, 2009, 4701.
31 S. Gendler, S. Segal, I. Goldberg, Z. Goldschmidt and M. Kol, *Inorg. Chem.*, 2006, **45**, 4783.
32 S. Groysman, E. Sergeeva, I. Goldberg and M. Kol, *Inorg. Chem.*, 2005, **44**, 8188.
33 L. M. Broomfield, Y. Sarazin, J. A. Wright, D. L. Hughes, W. Clegg, R. W. Harrington and M. Bochmann, *J. Organomet. Chem.*, 2007, **692**, 4603.
34 Z. Janas, T. Nerkowski, E. Kober, L. B. Jerzykiewicz and T. Lis, *Dalton Trans.*, 2012, **41**, 442.
35 R. K. Dean, S. L. Granville, L. N. Dawe, A. Decken, K. M. Hattenhauer and C. M. Kozak, *Dalton Trans.*, 2010, **39**, 548.
36 W. Clegg, M. G. Davidson, D. V. Graham, G. Griffen, M. D. Jones, A. R. Kennedy, C. T. O'Hara, L. Russoa and C. M. Thomson, *Dalton Trans.*, 2008, 1295.
37 P. A. van der Schaaf, M. P. Hogerheide, D. M. Grove, A. L. Spek and G. van Koten, *J. Chem. Soc., Chem. Commun.*, 1992, 1703.
38 T. J. Boyle, D. M. Pedrotty, T. M. Alam, S. C. Vick and M. A. Rodriguez, *Inorg. Chem.*, 2000, **39**, 5133.
39 J. S. Vilardo, P. E. Fanwick and I. P. Rothwell, *Polyhedron*, 1998, **17**, 769.
40 M.-H. Thibault and F.-G. Fontaine, *Dalton Trans.*, 2010, **39**, 5688.
41 C. Yu, L. Zhang and Z. Shen, *Eur. Polym. J.*, 2003, **39**, 2035.
42 N. Iwasa, S. Katao, J. Liu, M. Fujiki, Y. Furukawa and K. Nomura, *Organometallics*, 2009, **28**, 2179.
43 Ph. Dubois, N. Ropson, R. Jerome and Ph. Teyssie, *Macromolecules*, 1996, **29**, 1965.
44 H.-Y. Chen, B.-H. Huang and C.-C. Lin, *Macromolecules*, 2005, **38**, 5400.
45 W. M. Stevels, M. J. K. Ankone, P. J. Dijkstra and J. Feijen, *Macromolecules*, 1996, **29**, 8296.
46 W. Zhu, J. Ling and Z. Shen, *Polym. Bull.*, 2004, **52**, 185.
47 L. Zhang, Y. Niu, Y. Wang, P. Wang and L. Shen, *J. Mol. Catal. A: Chem.*, 2008, **287**, 1.
48 Y. A. Piskun, I. V. Vasilenko, S. V. Kostjuk, K. V. Zaitsev, G. S. Zaitseva and S. S. Karlov, *J. Polym. Sci., Part A: Polym. Chem.*, 2010, **48**, 1230.
49 Y. Yao, Y. Mu, A. Gao, Q. Su, Y. Liu and Y. Zhang, *Polymer*, 2008, **49**, 2486.
50 A. Kowalski, A. Duda and S. Penczek, *Macromolecules*, 2000, **33**, 689.
51 Ph. Dubois, R. Jacobs and R. Jerome, *Macromolecules*, 1991, **24**, 2266.
52 A. Kowalski, A. Duda and S. Penczek, *Macromolecules*, 2000, **33**, 689.
53 M. Sobczak and W. Kolodziejski, *Molecules*, 2009, **14**, 621.
54 J. E. Baez, A. M. Richa and A. M. Fernandez, *Macromolecules*, 2005, **38**, 1599.
55 SHELX97: G. M. Sheldrick, *Acta Crystallogr., Sect. A*, 2008, **64**, 112.
56 SIR92: A. Altomare, M. C. Burla, M. Camalli, G. Cascarano, C. Giacovazzo, A. Guagliardi and G. Polidori, *J. Appl. Crystallogr.*, 1994, **27**, 435.
57 DIRDIF99: P. T. Beurskens, G. Beurskens, R. de Gelder, S. Garcia-Granda, R. O. Gould, R. Israel and Jan M. M. Smits, *The DIRDIF-99 program system*, Crystallography Laboratory, University of Nijmegen, The Netherlands, 1998.
58 D. T. Cromer and J. T. Waber, *International Tables for X-ray Crystallography*, The Kynoch Press, Birmingham, England, 1974, vol. IV, Table 2.2 A.
59 J. A. Ibers and W. C. Hamilton, *Acta Crystallogr.*, 1964, **17**, 781.
60 D. C. Creagh and W. J. McAuley, *International Tables for Crystallography*, ed. A. J. C. Wilson, Kluwer Academic Publishers, Boston, 1992, vol C, Table 4.2.6.8, pp. 219–222.
61 D. C. Creagh and J. H. Hubbell, *International Tables for Crystallography*, ed. A. J. C. Wilson, Kluwer Academic Publishers, Boston, 1992, vol C, Table 4.2.4.3, pp. 200–206.
62 CrystalStructure 3.7.0: Crystal Structure Analysis Package, Rigaku and Rigaku/MSC (2000–2005). 9009 New Trails Dr. The Woodlands TX 77381 USA.
63 CRYSTALS Issue 10: J. Watkin, C. K. Prout, J. R. Carruthers and P. W. Betteridge, Chemical Crystallography Laboratory, Oxford, UK, 1996.
64 A. L. Spek, *J. Appl. Crystallogr.*, 2003, **36**, 7–13.